

Journal of Biomolecular Screening

<http://jbx.sagepub.com>

Label-Free and Real-Time Cell-Based Kinase Assay for Screening Selective and Potent Receptor Tyrosine Kinase Inhibitors Using Microelectronic Sensor Array

Josephine M. Atienza, Naichen Yu, Xiaobo Wang, Xiao Xu and Yama Abassi

J Biomol Screen 2006; 11; 634 originally published online Jul 20, 2006;

DOI: 10.1177/1087057106289334

The online version of this article can be found at:
<http://jbx.sagepub.com/cgi/content/abstract/11/6/634>

Published by:

 SAGE Publications

<http://www.sagepublications.com>

On behalf of:



Society for Biomolecular Sciences

Additional services and information for *Journal of Biomolecular Screening* can be found at:

Email Alerts: <http://jbx.sagepub.com/cgi/alerts>

Subscriptions: <http://jbx.sagepub.com/subscriptions>

Reprints: <http://www.sagepub.com/journalsReprints.nav>

Permissions: <http://www.sagepub.com/journalsPermissions.nav>

Citations (this article cites 39 articles hosted on the SAGE Journals Online and HighWire Press platforms):
<http://jbx.sagepub.com/cgi/content/refs/11/6/634>

Label-Free and Real-Time Cell-Based Kinase Assay for Screening Selective and Potent Receptor Tyrosine Kinase Inhibitors Using Microelectronic Sensor Array

JOSEPHINE M. ATIENZA, NAICHEN YU, XIAOBO WANG, XIAO XU, and YAMA ABASSI

Kinases are the 2nd largest group of therapeutic targets in the human genome. In this article, a label-free and real-time cell-based receptor tyrosine kinase (RTK) assay that addresses limitation of existing kinase assays and can be used for high-throughput screening and lead optimization studies was validated and characterized. Using impedance, growth factor-induced morphological changes were quantitatively assessed in real time and used as a measure of RTK activity. COS7 cells treated with epidermal growth factor (EGF) and insulin results in a rapid increase in cell impedance. Assessment of these growth factor-induced morphological changes and levels of receptor autophosphorylation using fluorescent microscopy and enzyme-linked immunosorbent assay, respectively, demonstrates that these changes correlate with changes in impedance. This assay was used to screen, identify, and characterize a potent EGF receptor inhibitor from a compound library. This report describes an assay that is simple in that it does not require intensive optimization or special reagents such as peptides, antibodies, or probes. More important, because the assay is cell based, the studies are done in a physiologically relevant environment, allowing for concurrent assessment of a compound's solubility, stability, membrane permeability, cytotoxicity, and off-target interaction effects. (*Journal of Biomolecular Screening* 2006:634-643)

Key words: impedance, cell-based assay, receptor tyrosine kinase, kinase, growth factor

INTRODUCTION

KINASES ARE ENZYMES that catalyze the transfer of a phosphate group from nucleoside triphosphates to an acceptor group. More than 500 different protein kinases have been identified, constituting ~1.7% of the human genome; of these, 17% are known to be tyrosine kinases (TKs).¹ The receptor tyrosine kinase (RTK) and nonreceptor forms (non-RTK) of TK mediate important cellular processes including proliferation, survival, differentiation, metabolism, motility, and gene expression.² It is therefore not surprising that deregulation of TK activity as a result of loss of control in its regulatory proteins or of mutations that increase expression of its transcript, protein, or ligand is implicated in numerous pathological conditions including cancer, inflammation, metabolism, and cardiovascular diseases.

RTKs are type I transmembrane receptor proteins that transmit extracellular signals intracellularly through the transfer of phosphate groups from adenosine triphosphate (ATP) to tyrosine residues on protein substrates. Among the well-studied RTKs are the epidermal growth factor receptor (EGFR/HER1) group that also includes HER2, HER3, and HER4.³ Disregulation of EGFR is implicated in the pathogenesis of many solid tumors, including breast, head-and-neck, non-small-cell lung, renal, ovarian, and colon cancer, in which it acts by promoting the proliferation and progression of malignant cells.^{4,5} Increased expression of HER2 or its amplification correlates with breast carcinoma progression and poor prognosis.^{6,7} Similar to other RTKs, the binding of its ligand, EGF, leads to activation and autophosphorylation of EGFR. These phosphorylated tyrosine residues serve as docking sites for intracellular adaptor proteins and kinases including Shc, Grb2, PLC γ , and PI3K.^{8,9} The binding of these proteins to EGFR couples the extracellular signal to a network of intracellular signaling pathways that control cell proliferation, survival, cytoskeletal changes, adhesion, motility, migration, and invasion.

The central role of RTKs in these cellular processes and their drugability has made them important and viable therapeutic targets. Numerous strategies including the use of peptides,

ACEA Biosciences, San Diego, California.

Received Oct 27, 2005, and in revised form Mar 28, 2006. Accepted for publication Apr 3, 2006.

Journal of Biomolecular Screening 11(6); 2006
DOI: 10.1177/1087057106289334

antibodies, small molecules, antisense, or small interfering RNA (siRNA) are being adapted to inhibit receptor tyrosine kinase activity. This has resulted in the development and approval of several inhibitors for kinases that include imatinib for Bcr-Abl/PDGFR/c-Kit, trastuzumab for HER2, erlotinib for EGFR, and bevacizumab for VEGFR. The importance of RTKs as therapeutic targets also led to the development of numerous screening platforms for the identification of inhibitors for RTK. These include antibody-based technologies such as AlphaScreen, time resolved-fluorescence resonance energy transfer (TR-FRET), fluorescence polarization, time-resolved fluorescence (TRF), scintillation proximity assay, Luminex, and enzyme-linked immunosorbent assay (ELISA) and non-antibody-based technologies such as incorporation of radioactivity, ATP consumption, and measurement of change of substrate size and charge. Although these technologies offer some advantages, they are limited by one or more of the following factors: complicated and tedious optimization steps, limited substrate capacity, assay component interference, and expensive assay components, all of which can affect the signal, throughput, time, and utility of the assay. Therefore, there is a need for an improved assay that addresses most of these limitations and concurrently provides an additional ability to assess a compound's toxicity, specificity, selectivity, potency, and effectiveness within a cellular context.

One of the intracellular pathways activated by RTK is the induction of immediate morphological changes, as exemplified by membrane ruffling, filopodia, and lamellipodia formations.¹⁰⁻¹³ EGF binding to EGFR induces these morphological changes through the activation of Rac and Rho, members of the Rho family of small GTPases.^{10,11} Using scanning electron microscopy (SEM), time-lapse imaging, or FRET-based imaging, several studies have assessed cell morphology as a sensitive assay for the integrated biological response elicited by EGF.¹⁴⁻¹⁷ However, the use of cell morphology as an output for a screen to identify inhibitors of growth factor receptors or of its downstream signaling pathways is hampered by the intractability of existing techniques used to measure morphological changes.

Taking advantage of the immediate morphological changes induced by RTKs, we report on the development and utility of a novel cell-based RTK assay that employs a sensor-based technology to quantitatively measure RTK-induced morphological changes using impedance. This method is based on the process of monitoring a cell behavior, referred to as electric cell-substrate impedance sensing.¹⁸ This has been used to assess cytotoxicity,^{19,20} cell attachment and spreading,^{21,22} migration,²³ and receptor activity.²⁴ Using this quantifiable parameter, we show that EGF-induced morphological changes in COS7 cells result in changes in impedance that correlate with levels of RTK activation. We also show that these responses are unique to each growth factor and are mediated by signaling pathways that regulate growth factor-induced morphological changes. Finally, we

demonstrate the 1st use of impedance as a quantitative measure of cell morphology to functionally screen, identify, and characterize RTK inhibitors and downstream signaling regulators.

MATERIALS AND METHODS

Cell culture and reagents

COS7 cells were acquired from ATCC (Manassas, VA). They were maintained in DMEM supplemented with 10% fetal bovine serum and incubated at 37 °C with 5% CO₂. EGF (Sigma, St. Louis, MO), EGF inhibitors including 4557W (4-(4-benzyloxyanilino)-6,7-dimethoxyquinazoline), compound 56 (4-[(3-bromophenyl)amino]-6,7-dimethoxyquinazoline), and BPIQII (8-[(3-bromophenyl)amino]-1H-imidazo[4,5-g]-quinazoline) and signaling inhibitors including U73122, bisindolylmaleimide I and wortmannin (Calbiochem, San Diego, CA), and LOPAC enzyme inhibitor ligand set (Sigma) were resuspended and stored according to the manufacturers' instructions. The LOPAC library contains compounds that inhibit a variety of enzymes including oxidases, phosphodiesterases, phosphatases, and kinases. Among the kinase inhibitors, the library contains inhibitors for TKs: tyrphostin AG879 (well number 20), genistein (well number 64), tyrphostin A9 (well number 10); protein kinase C: chelerythine chloride (well number 62), H-7 (well number 35), NPC-15437 (well number 37); MAP kinases: U0126 (well number 40), PD098059 (well number 48), SP600125 (well number 15); PI3K: LY-294002 (well number 16); and protein kinase A: HA-1004 (well number 54).

ELISA

Cells were plated on sensor plates at 1×10^4 cells per well and incubated overnight. During the day of the assay, cells were serum starved in DMEM supplemented with 0.25% bovine serum albumin (BSA) for a total of 4 h. If pretreated with inhibitors, cells were preincubated with inhibitors during the last hour of serum starvation and stimulated with growth factors for 15 min. After growth factor stimulation, cells were washed 2 times with cold phosphate-buffered saline (PBS) and lysed. ELISA (Biosource, Carlsbad, CA) assay to detect total EGFR, and phospho-EGFR (P-1068) was performed according to the manufacturer's instructions and read at 450 nm.

Immunocytochemistry

Cells were manipulated similar to ELISA except for the following changes. Cells were pretreated with 10 μ M EGFR inhibitor, 4557W, or vehicle for 1 h and stimulated with 25 ng/mL EGF. After 0, 5, and 20 min of EGF treatment, cells were washed once with PBS and fixed in 4% paraformaldehyde for 15 min at 37 °C. Fixed cells were washed with PBS twice and permeabilized with 0.1% Triton X-100 for 10 min. Permeabilized

cells were washed with PBS, blocked with 3% BSA in PBS-T (PBS with 0.1% Triton X-100) for 1 h at room temperature. To probe for Rac, cells were treated with mouse anti-Rac antibody (Sigma) and probed with tetramethylrhodamine isothiocyanate-conjugated antimouse secondary antibody (Sigma). Cells were then probed with fluorescein isothiocyanate-conjugated phalloidin (Sigma) to probe for actin. For each experimental well, 4 individual fields were measured using a digital camera attached to a Nikon fluorescent microscope.

Data analysis

All dose-response curves were generated by plotting the average of percent of controls with standard deviations versus ligand or inhibitor concentrations. The average percentage control was calculated either relative to the positive control, samples treated with growth factor plus vehicle, or to the negative control, samples untreated with growth factor, of quadruplicate samples and fitted using a 4-parameter logistic nonlinear regression equation. The EC_{50} for ligands and IC_{50} for inhibitors were determined from the fitted curve generated by *XLfit* 4.0.

Impedance measurement of cell behavior

Throughout the experimental process, cells were continually monitored, and changes in impedance were acquired with the ACEA (San Diego, CA) real-time cell electronic sensing (RT-CES) system. Cells were manipulated similar to ELISA except for the following changes. COS7 cells were pretreated with vehicle, DMSO, or the indicated inhibitor and then treated with 25 ng/mL of growth factor. After ligand treatment, data acquisition of changes in impedance was done every minute for up to 5 h.

The principle of impedance measurement using the RT-CES has been previously described.¹⁹ Briefly, gold sensors or electrodes are arrayed on the bottom of culture wells. The electronic impedance of these sensors is determined primarily by the ion environment at the electrode/solution interface and the bulk solution. When cells are cultured on these sensors, a change in the local ionic environment at the electrode/solution interface occurs, leading to an increase in the sensor impedance. Furthermore, a change in the amount of coverage of these sensors as a result of changes in cell morphology or cell number can also lead to changes in the local ionic environment at the electrode/solution interface resulting in impedance changes. The RT-CES system measures these changes in impedance and displays it as a parameter called cell index. Cell index was calculated according to the formula

$$CI = \max_{i=1, \dots, N} \left(\frac{R_{cell}(f_i)}{R_0(f_i)} - 1 \right),$$

where the number of the frequency points at which the impedance is measured (e.g., $N = 3$ for 10 kHz, 25 kHz, and 50 kHz),

and $R_0(f)$ and $R_{cell}(f)$ are the frequency electrode resistance without cells or with cells present in the wells, respectively.

RESULTS

Growth factors induce specific morphological changes that can be measured by impedance

The microsensors arrayed on the bottom of the plates used in these experiments acutely measure changes in impedance. This is determined by changes in the ionic composition in the solution/sensor interface resulting from changes in cellular adhesion or sensor area covered by cells due to increased cell number or morphological changes.¹⁸ To determine if impedance can be used to measure growth factor-induced changes in cell behavior, COS7 cells, which endogenously express several RTKs, were treated with EGF and insulin, and cell index, which is a measure of impedance change, was continuously recorded. Addition of 25 ng/mL of EGF or insulin produced a distinctive pattern of cell index change (**Fig. 1A**). This is characterized by an immediate and very rapid increase in cell index, with the maximum cell index change (peak cell index) occurring within 20 min. For EGF, this is followed by a relatively rapid decrease in cell index within an hour. However, for insulin, the rate of decrease occurs even slower and returns to baseline after several hours. To determine the specificity of these responses, COS7 cells were pretreated for 1 h with 10 μ M of EGFR inhibitor, 4557W.²⁵ The rapid and immediate rise in cell index as a result of EGF, but not of insulin, was blocked by 4557W (**Fig. 1B**). The absence of the 4557W effect on the insulin response demonstrates that the unique changes in impedance are a result of the specific response to EGF.

Growth factor treatment of cells can induce several molecular and cellular responses including the induction of morphological changes characterized by lamellipodia, membrane ruffle, and filopodia formations.^{10,12,13} Growth factor-induced lamellipodia formation is mediated by small GTPases including Rac¹¹ and is characterized by rapid actin polymerization leading to dynamic reorganization of the cytoskeleton, which is manifested as thin membrane protrusions that extend and retract continuously. To demonstrate that the change in cell index, which is a measure of change in impedance, correlates with growth factor-induced morphological change, cells were stained with phalloidin and an antibody against Rac. Cells treated with 25 ng/mL of EGF showed an increase in cell area as a result of lamellipodia formation as early as 5 min and persists for at least 20 min (**Fig. 2A-F**). The EGF-induced membrane protrusions stained positively with phalloidin, confirming actin polymerization and remodeling dynamically occurring in these structures. Intense staining of Rac was also observed at the edge of these membrane protrusions. These morphological changes correlate temporally with the onset and peak of cell index after EGF treatment (**Fig. 1A**).

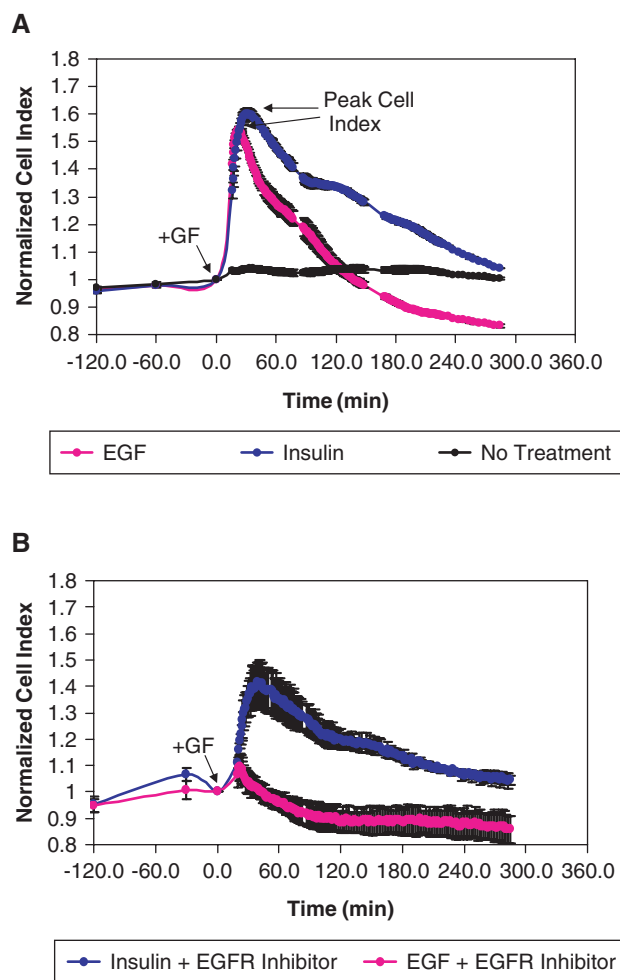


FIG. 1 Cell index curves of COS7 cells treated with growth factors, insulin or epidermal growth factor (EGF). (A) COS7 cells treated with insulin or EGF (arrow, +GF) showed unique responses characterized by a sharp and transient increase in cell index, with peak cell index (arrow) occurring within 30 min, and followed by a slow decrease in cell index. Insulin-treated cells showed a slower rate of decrease in cell index relative to EGF-treated cells. (B) COS7 cells were pretreated for 1 h with 10 μ M EGF receptor (EGFR) inhibitor, 4557W, or vehicle prior to growth factor treatment. Cells pretreated with 4557W and stimulated with EGF did not show the transient increase in cell index, whereas the insulin response remained intact. Each curve is an average of $n = 4 \pm$ SD.

The specificity of this response is supported by the significant inhibition of morphological changes and Rac translocation in cells pretreated with the EGFR inhibitor, 4557W (Fig. 2G-H). This is consistent with the absence of changes in cell index measured in these samples (Fig. 1B). These observations demonstrate that the growth factor-induced increase in impedance correlates with growth factor-induced morphological changes, which are characterized by an increase in cell surface area covering the sensors.

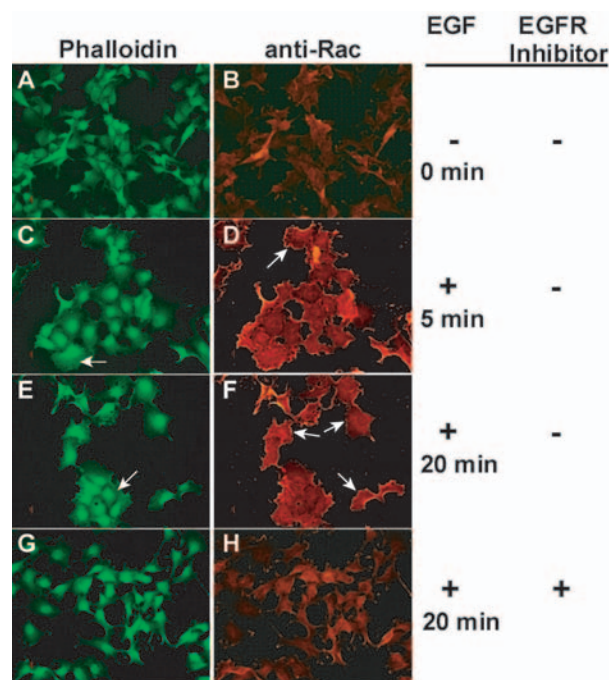


FIG. 2. Fluorescent microscopy images of COS7 cells treated with EGF and \pm 4557W. (A, B) Cells pretreated with vehicle alone and before treatment with epidermal growth factor (EGF) appeared relatively small and exhibited low Rac staining. (C, D) Cells treated with 25 ng/mL EGF showed rapid formation of lamellipodia (arrows) within 5 min as observed by an increase in the cell size. Intense staining of actin and Rac is observed at the lamellipodia and its edge (arrows), respectively. (E, F) These changes continue to be observed at 20 min. (G, H) Cells pretreated with 10 μ M 4557W showed a phenotype similar to that of cells before treatment with EGF (A, B). They appeared smaller, and a decreased staining for Rac is observed.

Changes in impedance as a result of growth factor-induced morphological changes are a quantitative measure of kinase activity

To determine if the EGF-induced impedance changes correlate with EGFR activation, cells were treated with a range of EGF concentrations while impedance and levels of receptor tyrosine autophosphorylation were concurrently measured. Treatment of COS7 cells with increasing concentrations of EGF resulted in a dose-dependent increase in measured impedance change as reflected by the increase in normalized cell index over the time course of measurement (Fig. 3A). Concurrently, cells were treated for 15 min with EGF lysed, and levels of phosphorylation on Tyr1068 (pTyr1068), measured by ELISA. Similar to the dose-dependent increase in cell index, an increase in levels of EGFR phosphorylation were also observed with treatment of increasing EGF concentrations (Fig. 3B). The correlation of EGFR activation and changes in impedance is supported by the similar EC_{50} values calculated

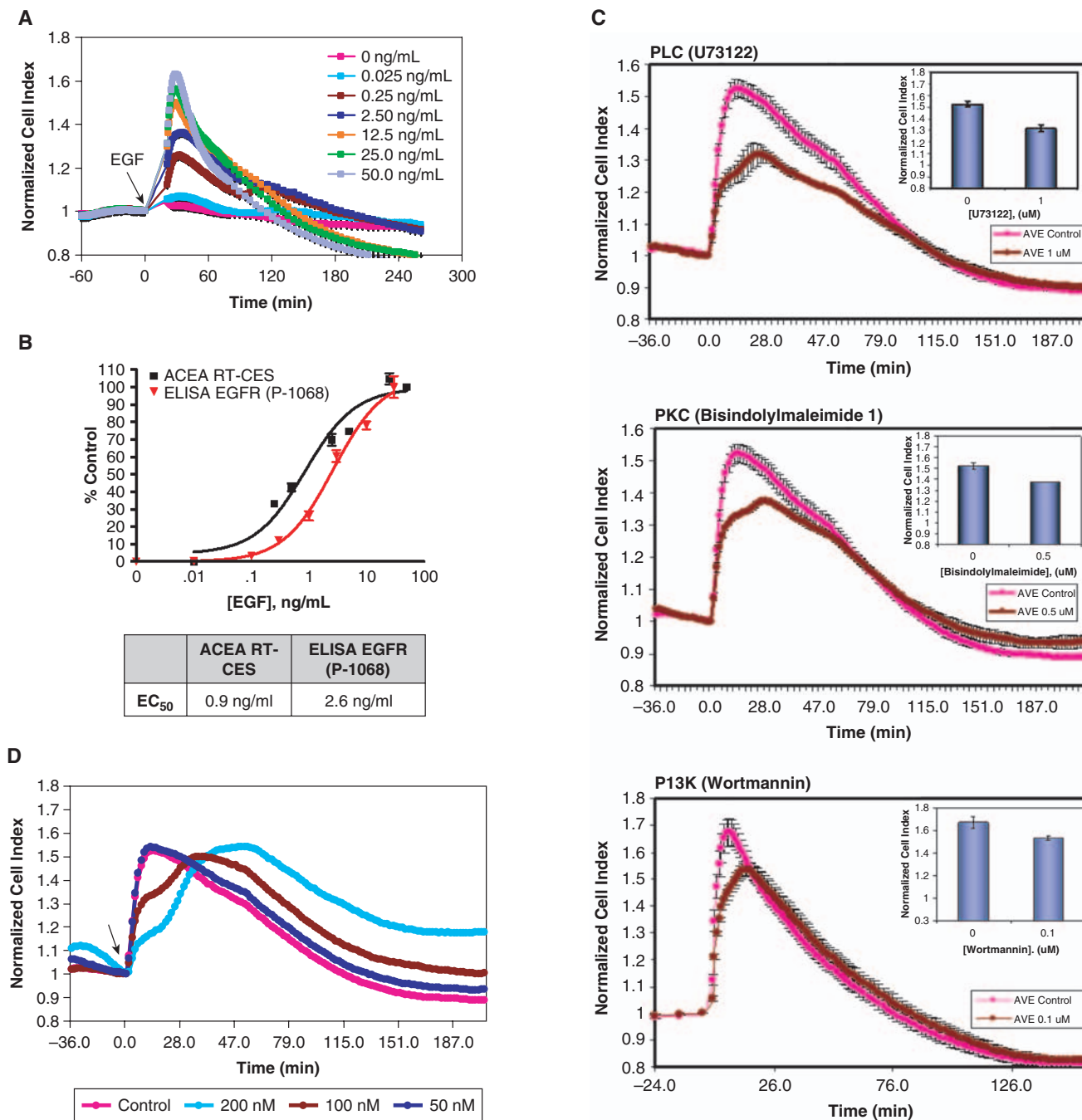


FIG. 3. Measurement of dose-dependent cell index change, levels of phosphorylation of epidermal growth factor receptor (EGFR), and effects on downstream signaling pathways induced by EGF. **(A)** Treatment with increasing concentrations of EGF resulted in increasing magnitude of cell index change. **(B)** Comparison of dose-response curves generated from real-time cell electronic sensing (RT-CES) and enzyme-linked immunosorbent assay (ELISA). Peak cell index from impedance curves and levels of pTyr1068 of EGFR for each ligand concentration treatments were measured, and the percent of increase relative to untreated control samples was determined and plotted as percent of control versus EGF concentrations. Curve-fitting and EC_{50} values were calculated from dose-response curves using *XLfit*. **(C)** Real-time measurements of effect of various intracellular signaling inhibitors on EGF-induced cell index change. Cells treated with U73122, bisindolylmaleimide I, and wortmannin decreased the peak cell index of the curve. Inset bar graphs represent peak cell index values of each curve. Each curve is an average of $n = 4 \pm SD$. **(D)** Real-time measurement of cell index change of cells pretreated with different concentrations of latrunculin. A delay in the peak cell index was observed with increasing concentrations of latrunculin up to 200 nM, whereas the rate of change of cell index for the rest of the curves remained the same.

from the EGF dose-response curves of cell index and pTyr1068 measurements (**Fig. 3B**). This experiment demonstrates that the level of impedance change quantitatively reflects the level of EGFR activation.

EGF activation of EGFR results in subsequent stimulation of downstream signaling pathways including PLC γ , PKC, and PI3K pathways.^{8,9} These pathways are known to mediate growth factor-induced cytoskeletal changes downstream of activated EGFR.²⁶⁻³¹ Because the EGF-induced impedance change is a result of morphological changes, the role of these pathways in mediating the EGF-induced cell impedance changes was examined. Small-molecule inhibitors for these pathways are reported to inhibit other kinases. Therefore, we used reported concentrations that would produce the least amount of cross-inhibition.³² COS7 cells were pretreated with 1 μ M of U73122, an inhibitor of agonist-induced PLC γ activation; 0.5 μ M of bisindolylmaleimide I, a highly selective PKC inhibitor; and 0.1 μ M of wortmannin, a potent, selective, and irreversible PI3K inhibitor. Interestingly, U73122, bisindolylmaleimide I, and wortmannin reduced the peak cell index (**Fig. 3C**). Studies show that signaling through these pathways lead to the activation of small GTPases, which in turn induces actin polymerization.³³ To determine if the EGF-induced impedance changes result from actin polymerization, cells were pretreated for 1 h with increasing concentrations of latrunculin, a reversible inhibitor of actin polymerization.^{34,35} Consistent with the reversible nature of latrunculin, a delayed increase in the peak cell index that is directly related to the latrunculin dose was observed after EGF treatment (**Fig. 3D**). These data implicate the activation of cognate receptor and canonical downstream pathways that mediate cytoskeletal reorganization in the changes in impedance after growth factor treatment.

Screening and characterization of potency and selectivity of EGFR inhibitor using impedance

Using SEM, time-lapse imaging, or FRET-based imaging, several studies have assessed cell morphology as a sensitive assay for the integrated biological response elicited by EGF.¹⁴⁻¹⁷ To demonstrate the utility of impedance, which quantitatively measures changes in cell morphology, as a readout to identify potent inhibitors of EGFR or its activated downstream signaling pathways, Sigma's enzyme inhibitor Ligand Set was screened. This is a collection of 80 diverse small organic compounds that have drug-like properties. In addition, 4557W, a potent EGFR inhibitor, was added to the collection. Prior to initiating the screen, the assay performance was quantitatively evaluated. A Z' factor of 0.6 was determined, providing evidence for the robustness, consistency, and signal strength of the assay. COS7 cells were pretreated for 1 h with a single concentration of the inhibitors and stimulated with EGF. This screening was

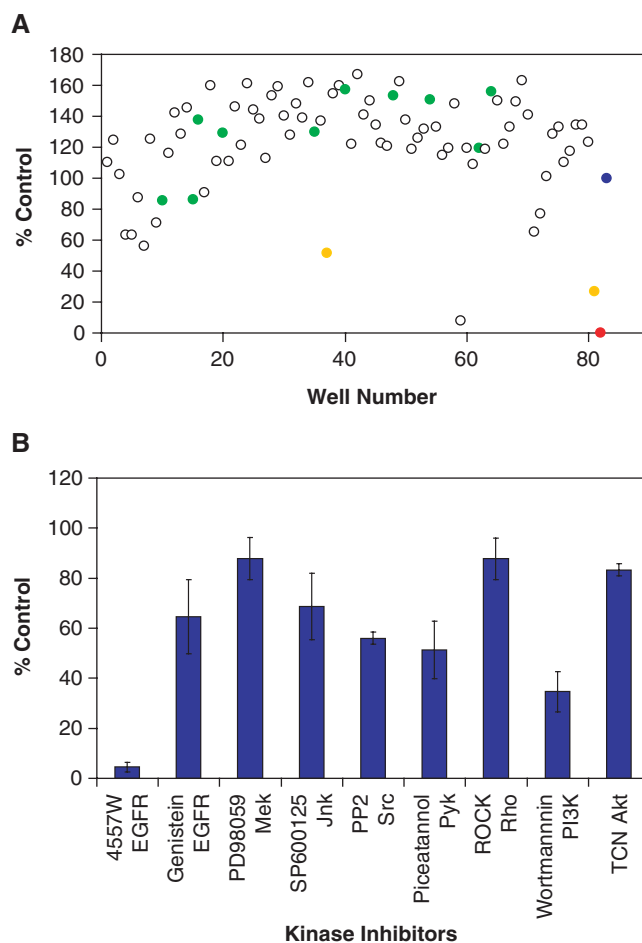


FIG. 4. Small-molecule inhibitor screen for epidermal growth factor receptor (EGFR) inhibitors using real-time cell electronic sensing. **(A)** Graphical representation of a screen of 81 compounds mostly from Sigma's enzyme inhibitor Ligand Set. Each inhibitor was screened at a single concentration between 5 and 10 μ M. The peak cell index was measured for each sample, and the percentage of inhibition of EGF-induced cell index change was determined and plotted as percent of control versus well position of inhibitors. Screening of the inhibitor library was conducted twice. Red and blue dots represent negative (cells without EGF but with vehicle) and positive controls (cells with EGF and vehicle), respectively; yellow dots represent inhibitors that were considered hits; and green dots represent kinase inhibitors in the library (see the "Material and Methods" section for a list of kinases and well positions). **(B)** Bar graph of inhibition of EGF-induced cell index change by a collection of known kinase inhibitors. Normalized peak cell index was plotted as percent of control (cells with EGF and vehicle) versus inhibitors.

repeated to verify hits initially identified. Using >50% inhibition of positive control as the cutoff for subsequent analysis, 2 compounds were consistently identified that potently inhibit the cell index change induced by EGF (**Fig. 4A**). These compounds include NPC-15437, a PKC inhibitor, and 4557W, the potent EGFR inhibitor. To further test its utility in identifying a potent EGFR inhibitor, a small collection of small-molecule

kinase inhibitors that are chemically and functionally similar was also examined. Interestingly, this collection of kinase inhibitors showed 4557W to be the only molecule that potently inhibited the EGF-mediated cell index change, verifying results of the initial screen (**Fig. 4B**).

To characterize the potency and activity of 4557W, its dose-dependent effect on EGF-induced impedance change and levels of phosphorylation of EGFR were determined using RT-CES and ELISA, respectively. Pretreatment with increasing concentrations of 4557W resulted in a dose-dependent inhibition of EGF-induced morphological changes as measured by the decreasing peak cell index (**Fig. 5A**). To determine if this decrease in impedance is due to inhibition of the activation of EGFR, levels of EGFR pTyr1068 were measured. Pretreatment with increasing concentrations of 4557W also resulted in a dose-dependent inhibition of EGF-induced phosphorylation of Tyr1068. The correlation of these 2 outputs is marked by the same trends in the dose-response plots, and more importantly, the IC_{50} values of 144 nM calculated from ELISA were similar to IC_{50} values of 364 nM derived from measuring cell index change (**Fig. 5B**). This confirms the earlier conclusion that the EGF-induced changes in impedance are specific and that in this case, quantitatively reflect the level of inhibition of the receptor.

Effect of representative RTK ligands such as platelet-derived growth factor form AB (PDGF-AB), basic fibroblast growth factor (bFGF), insulin, and hepatocyte growth factor (HGF) were additionally examined on primary and established cell lines, and changes in impedance were observed as a result of treatment of these ligands (data not shown). In addition to EGF, insulin and HGF were also observed to induce significant cell index change in COS7 cells. Because most kinase inhibitors are ATP competitors and the ATP binding site among kinases is highly conserved, it is important to functionally define or verify the selectivity of kinase inhibitors. To partially define the selectivity of 4557W for the inhibition of EGFR, the effect of this inhibitor on insulin- and HGF-induced cell morphological changes was examined. COS7 cells were pretreated with different concentrations of 4557W and then stimulated with insulin or HGF. Based on the measured cell index change, 4557W did not inhibit the insulin- or HGF-induced morphological changes at concentrations up to 30 μ M (**Fig. 5C**). This selectivity of 4557W is consistent with and supplements reported data of its selectivity for the EGFR subfamily versus a range of isolated kinases.²⁵

The sensitivity of this assay in quantitatively measuring EGFR activity is underscored by its ability to detect cellular changes induced by low levels of ligand or inhibitor. To further explore the sensitivity of the assay, several EGF inhibitors were characterized, and rank potency was determined. COS7 cells were pretreated with various EGFR inhibitors, compound 56, 4557W, and BPIQII, for 1 h and then treated with EGF. The peak cell index for each concentration of inhibitors was determined

and plotted as percentage control against the inhibitor concentrations. All 3 dose-response curves were plotted, and IC_{50} values of 0.186, 0.303, and 1.584 μ M were derived for compound 56, 4557W, and BPIQII, respectively (**Fig. 5D**). However, using in vitro kinase assay, IC_{50} values of 0.006 nM, 0.008 nM, and 20 nM were derived from compound 56, BPIQII, and 4557W, respectively.^{25,36,37} Interestingly, different rank potencies were derived from these compounds using in vitro and cell-based kinase assays. These differences can be attributed to compound features, which, among other things, include membrane permeability, stability in the presence of serum, binding affinity at intracellular ATP concentrations, and mode of action that can not be solely assessed in an in vitro kinase assay.

DISCUSSION

Kinases play a fundamental role in numerous cellular processes. Their aberrant expressions in multiple disease states, drugability, and the effectiveness of recently approved kinase inhibitors have made them an even more attractive target for therapeutic intervention. In this report, we demonstrate and validate the use of impedance to quantitatively measure morphological changes induced by RTKs. The changes in impedance correlate with RTK activity, are specific to each growth factor, and are mediated by signaling pathways that regulate growth factor-induced morphological changes. In addition, we demonstrate the 1st use of impedance as a quantitative measure of cell morphology to functionally screen, identify, and characterize RTK inhibitors and downstream signaling regulators.

Growth factors and their kinase receptors activate a variety of intracellular signaling pathways that lead to numerous cellular responses including reorganization of the actin cytoskeleton and morphological changes that include lamellipodia formation.^{2,10,11} In this report, we show that the kinetics of impedance change as a result of EGF treatment correlates temporally with the observed lamellipodia formation on these cells. EGF treatment of COS7 cells results in an immediate increase in cell index, with the peak response occurring within 20 min (**Fig. 1A**). These measurements correlate with the increase in cell area due to lamellipodia formation, which is observed as early as 5 min and lasting up to 20 min (**Fig. 2**). These experiments are supported by reports using time-lapse imaging in which the onset of lamellipodia formation was observed to occur within 1 min and persist for approximately 20 min after EGF treatment.¹⁷ In addition, we show that these changes in impedance as a result of cell response to EGF are specific. Pretreatment of cells with 4557W, an EGFR inhibitor, inhibited the EGF and not the insulin-induced cell index (**Fig. 1B**) or morphological changes (**Fig. 2G, H**).

The binding of EGF to EGFR results in the autophosphorylation of tyrosine residues, which leads to the activation of the receptor³⁸ and its downstream signaling pathways. Treatment

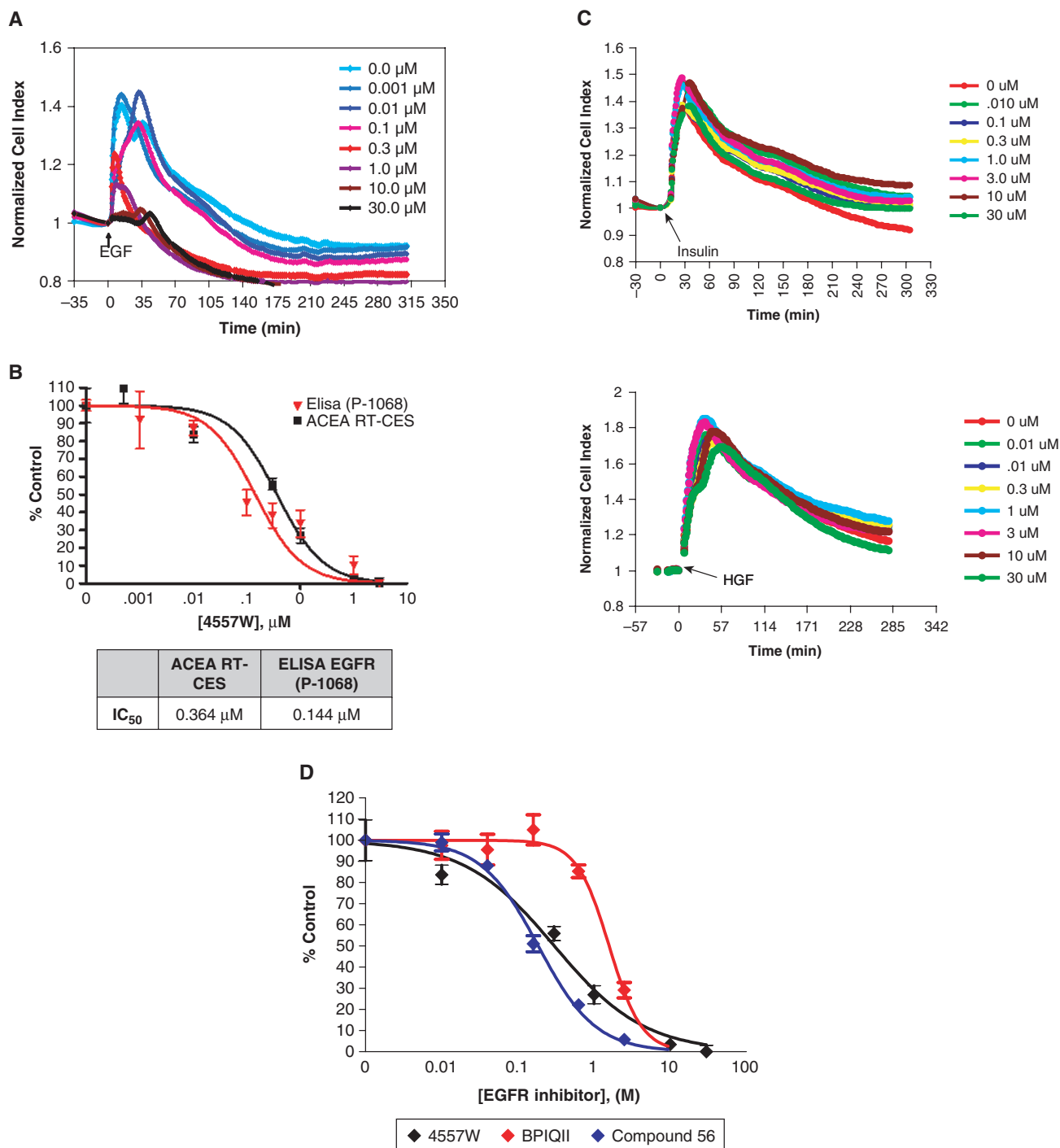


FIG. 5. Characterization of potency and selectivity of epidermal growth factor receptor (EGFR) inhibitor, 4557W, using real-time cell electronic sensing (RT-CES). **(A)** Real-time measurements of changes in impedance as a result of treatment with increasing concentrations of 4557W. Increasing concentrations of 4557W resulted in a decreasing magnitude of cell index change over time. **(B)** Comparison of dose-response curves generated from RT-CES and enzyme-linked immunosorbent assay (ELISA). The peak cell index from impedance curves and the levels of pTyr1068 of EGFR for each inhibitor concentration treatments were determined, and the percentage of inhibition of EGF-induced cell index change or levels of pTyr1068 was plotted as percent of control versus 4557W concentrations. Curve-fitting and IC₅₀ values were calculated from dose-response curves using *XLfit*. **(C)** Assessment of selectivity of 4557W for EGFR. The changes in cell index induced by insulin or hepatocyte growth factor (HGF) were not decreased by 4557W up to concentrations of 30 μM. **(D)** Various potent EGFR inhibitors, BPIQII (red) and compound 56 (blue), were additionally tested using RT-CES, and IC₅₀ values were determined and compared to 4557W (black). Each curve is an average of *n* = 4 ± SD.

of COS7 cells with either increasing concentrations of EGF or EGFR inhibitor resulted in a dose-dependent increase or decrease, respectively, of phosphorylation or cell index change (Figs. 3B, 5B). Among the many intracellular signaling pathways activated by EGFR, the activations of PLC γ , PKC, and PI3K are known to be primarily implicated in the EGF-induced lamellipodia formation.²⁶⁻³¹ Pretreatment with inhibitors against these pathways resulted in partial inhibition of the EGF-induced cell index change. This is consistent with published reports showing that treatment of cells with a PI3K inhibitor, wortmannin,³⁹ or with a small-molecule inhibitor against PLC γ , U73122,¹⁷ results in the inhibition of the rapid reorganization of the actin cytoskeleton in response to EGF. Because some of these inhibitors are known to inhibit other kinases, we took careful consideration in using concentrations that would prevent these cross-inhibitions in our experiments. For instance, 1 μ M of bisindolylmaleimide in an in vitro kinase assay inhibits 50% of GSK3 and 15% of PDK1 while inhibiting 96% of PKC α activity.³² In contrast, our study used 50% less bisindolylmaleimide I and was done in the context of a cell-based assay that conventionally requires a higher concentration. Therefore, at the concentration used in our experiment, we can be confident that the effect of bisindolylmaleimide I is due to the inhibition of PKC α . In addition, we used a validated concentration of wortmannin to inhibit PI3K.³² The rapid reorganization of the actin cytoskeleton induced by these pathways is mediated by the Rho family of small GTPases, which includes Rac, Cdc42, and Rho.³³ The intense staining of Rac at the edge of prominent membrane ruffles is consistent with reports demonstrating EGF-induced Rac translocation to the membrane (Fig. 2).¹⁷ Bright staining with phalloidin and a delayed increase in EGF-induced cell index change due to pretreatment with latrunculin confirms the presence of rapid actin remodeling. Although a need for a further elucidation of the contributing molecular mechanisms underlying each phase of the cell index curve is still necessary, these data nonetheless implicate the activation of the cognate receptor and canonical downstream pathways in mediating the cytoskeletal reorganization involved in changes in impedance after growth factor treatment.

Several studies have assessed cell morphology as a sensitive assay for the integrated biological response elicited by EGF.¹⁴⁻¹⁷ However, the use of cell morphology as an output for a screen to identify inhibitors of growth factor receptors or of its downstream signaling pathways is hampered by the intractability of current techniques used to measure morphological changes. In addition, other conventional cell-based RTK assays such as proliferation or ELISA require several days to perform and expensive special reagents. In this article, we present a label-free, cell-based RTK assay that uses impedance to quantitatively measure growth factor-induced morphological changes as a measure of RTK activation. We demonstrated the utility of this cell-based assay in screening both diverse and structurally similar libraries. Both screens identified the same potent inhibitor of EGFR and a downstream signaling pathway inhibitor. Although

the size of these libraries is small, the result nonetheless demonstrates the assay method's reproducibility, sensitivity, and utility in identifying potent inhibitors even in a compound set containing structurally and functionally similar compounds. Using this RTK assay, we characterized the potency and selectivity of 4557W, the EGFR inhibitor identified from the screen, and showed functionally that it had IC₅₀ values comparable to ELISA IC₅₀ and minimal activity against c-Met and the insulin receptor, receptor for HGF and insulin, respectively.

Cell-based assays are increasingly being used at multiple points during small molecule development including at the early stage of high-throughput screening (HTS). This is particularly necessary in studies in which targets are difficult to express, recombinant protein products prohibitively expensive, or analysis limited to the use of primary cells. These cases necessitate the use of an assay that is robust, specific, and easy to set up and does not require expensive and special reagents. In this report, we validated and characterized an RTK assay that possesses these features and can be used for HTS and also lead optimization studies. The assay is simple in that it does not require extensive optimization or special reagents such as peptides, antibodies, or special probes. It is conducted in a label-free environment and therefore is not subjected to small molecule interference or probe limitations. The assay is sensitive in that it responds to low concentrations of inhibitor and ligand. It is also specific enough that it can be performed on cell lines expressing endogenous levels of the receptor. The sensitivity and the specificity of the response of the assay also allows for its use in downstream small-molecule structure-activity relationship studies, whereas the real-time component of the assay allows its use in determining optimal scheduling and combinatorial treatment. Finally, because the assay is cell based, the studies are done in a physiologically relevant environment allowing for concurrent assessment of a compound's solubility, stability, membrane permeability, cytotoxicity, off-target interaction effects, and potential mode of action. This provides for increased efficiency in evaluation and development of compounds at early points of the drug development pipeline.

REFERENCES

1. Manning G, Whyte DB, Martinez R, Hunter T, Sudarsanam S: The protein kinase complement of the human genome. *Science* 2002;298:1912-1934.
2. Schlessinger J: Cell signaling by receptor tyrosine kinases. *Cell* 2000; 103:211-225.
3. Ullrich A, Coussens L, Hayflick JS, Dull TJ, Gray A, Tam AW, et al: Human epidermal growth factor receptor cDNA sequence and aberrant expression of the amplified gene in A431 epidermoid carcinoma cells. *Nature* 1984;309:418-425.
4. Nicholson RI, Gee JM, Harper ME: EGFR and cancer prognosis. *Eur J Cancer* 2001;37(Suppl 4):S9-S15.
5. Salomon DS, Brandt R, Ciardiello F, Normanno N: Epidermal growth factor-related peptides and their receptors in human malignancies. *Crit Rev Oncol Hematol* 1995;19:183-232.

6. Slamon DJ, Clark GM, Wong SG, Levin WJ, Ullrich A, McGuire WL: Human breast cancer: correlation of relapse and survival with amplification of the HER-2/neu oncogene. *Science* 1987;235:177-182.
7. Lohrisch C, Piccart M: HER2/neu as a predictive factor in breast cancer. *Clin Breast Cancer* 2001;2:129-135.
8. Gschwind A, Fischer OM, Ullrich A: The discovery of receptor tyrosine kinases: targets for cancer therapy. *Nat Rev Cancer* 2004;4:361-370.
9. Pawson T, Schlessinger J: SH2 and SH3 domains. *Curr Biol* 1993;3:434-442.
10. Ridley AJ, Hall A: The small GTP-binding protein rho regulates the assembly of focal adhesions and actin stress fibers in response to growth factors. *Cell* 1992;70:389-399.
11. Ridley AJ, Paterson HF, Johnston CL, Diekmann D, Hall A: The small GTP-binding protein rac regulates growth factor-induced membrane ruffling. *Cell* 1992;70:401-410.
12. Hall A: Rho GTPases and the actin cytoskeleton. *Science* 1998;279:509-514.
13. Chinkers M, McKanna JA, Cohen S: Rapid induction of morphological changes in human carcinoma cells A-431 by epidermal growth factors. *J Cell Biol* 1979;83:260-265.
14. Miyata Y, Nishida E, Koyasu S, Yahara I, Sakai H: Protein kinase C-dependent and -independent pathways in the growth factor-induced cytoskeletal reorganization. *J Biol Chem* 1989;264:15565-15568.
15. Welsh JB, Gill GN, Rosenfeld MG, Wells A: A negative feedback loop attenuates EGF-induced morphological changes. *J Cell Biol* 1991;114:533-543.
16. Yip SC, El-Sibai M, Hill KM, Wu H, Fu Z, Condeelis JS, et al: Overexpression of the p110beta but not p110alpha isoform of PI 3-kinase inhibits motility in breast cancer cells. *Cell Motil Cytoskeleton* 2004;59:180-188.
17. Kurokawa K, Itoh RE, Yoshizaki H, Nakamura YO, Matsuda M: Coactivation of Rac1 and Cdc42 at lamellipodia and membrane ruffles induced by epidermal growth factor. *Mol Biol Cell* 2004;15:1003-1010.
18. Giaever I, Keese CR: Monitoring fibroblast behavior in tissue culture with an applied electric field. *Proc Natl Acad Sci U S A* 1984;81:3761-3764.
19. Solly K, Wang X, Xu X, Strulovici B, Zheng W: Application of real-time cell electronic sensing (RT-CES) technology to cell-based assays. *Assay Drug Dev Technol* 2004;2:363-372.
20. Xing JZ, et al: Dynamic monitoring of cytotoxicity on microelectronic sensors. *Chem Res Toxicol* 2005;18:154-161.
21. Wegener J, Keese CR, Giaever I: Electric cell-substrate impedance sensing (ECIS) as a noninvasive means to monitor the kinetics of cell spreading to artificial surfaces. *Exp Cell Res* 2000;259:158-166.
22. Atienza JM, Zhu J, Wang X, Xu X, Abassi Y: Dynamic monitoring of cell adhesion and spreading on microelectronic sensor arrays. *J Biomol Screen* 2005;10:795-805.
23. Keese CR, Bhawe K, Wegener J, Giaever I: Real-time impedance assay to follow the invasive activities of metastatic cells in culture. *Biotechniques* 2002;33:842-844, 846, 848-850.
24. Ciambone GJ, Liu VF, Lin DC, McGuinness RP, Leung GK, Pitchford S: Cellular dielectric spectroscopy: a powerful new approach to label-free cellular analysis. *J Biomol Screen* 2004;9:467-480.
25. Cockerill S, Stubberfield C, Stables J, Carter M, Guntrip S, Smith K, et al: Indazolylamino quinazolines and pyridopyrimidines as inhibitors of the EGFR and C-erbB-2. *Bioorg Med Chem Lett* 2001;11:1401-1405.
26. Chen P, Murphy-Ullrich JE, Wells A: A role for gelsolin in actuating epidermal growth factor receptor-mediated cell motility. *J Cell Biol* 1996;134:689-698.
27. Wells A, Ware MF, Allen FD, Lauffenburger DA: Shaping up for shipping out: PLCgamma signaling of morphology changes in EGF-stimulated fibroblast migration. *Cell Motil Cytoskeleton* 1999;44:227-233.
28. Rodriguez-Viciano P, Warne PH, Khwaja A, Marte BM, Pappin D, Das P, et al: Role of phosphoinositide 3-OH kinase in cell transformation and control of the actin cytoskeleton by Ras. *Cell* 1997;89:457-467.
29. Wennstrom S, Hawkins P, Cooke F, Hara K, Yonezawa K, Kasuga M, et al: Activation of phosphoinositide 3-kinase is required for PDGF-stimulated membrane ruffling. *Curr Biol* 1994;4:385-393.
30. Kotani K, Yonezawa K, Hara K, Ueda H, Kitamura Y, Sakaue H, et al: Involvement of phosphoinositide 3-kinase in insulin- or IGF-1-induced membrane ruffling. *Embo J* 1994;13:2313-2321.
31. Sun XG, Rotenberg SA: Overexpression of protein kinase Calpha in MCF-10A human breast cells engenders dramatic alterations in morphology, proliferation, and motility. *Cell Growth Differ* 1999;10:343-352.
32. Davies SP, Reddy H, Caivano M, Cohen P: Specificity and mechanism of action of some commonly used protein kinase inhibitors. *Biochem J* 2000;351:95-105.
33. Burridge K, Wennerberg K: Rho and Rac take center stage. *Cell* 2004;116:167-179.
34. Ayscough KR, et al: High rates of actin filament turnover in budding yeast and roles for actin in establishment and maintenance of cell polarity revealed using the actin inhibitor latrunculin-A. *J Cell Biol* 1997;137:399-416.
35. Morton WM, Ayscough KR, McLaughlin PJ: Latrunculin alters the actin-monomer subunit interface to prevent polymerization. *Nat Cell Biol* 2000;2:376-378.
36. Bridges AJ, Zhou H, Cody DR, Rewcastle GW, McMichael A, Showalter HD, et al: Tyrosine kinase inhibitors. 8. An unusually steep structure-activity relationship for analogues of 4-(3-bromoanilino)-6,7-dimethoxyquinazoline (PD 153035), a potent inhibitor of the epidermal growth factor receptor. *J Med Chem* 1996;39:267-276.
37. Rewcastle GW, Palmer BD, Bridges AJ, Showalter HD, Sun L, Nelson J, et al: Tyrosine kinase inhibitors. 9. Synthesis and evaluation of fused tricyclic quinazoline analogues as ATP site inhibitors of the tyrosine kinase activity of the epidermal growth factor receptor. *J Med Chem* 1996;39:918-928.
38. Soler C, Beguinot L, Carpenter G: Individual epidermal growth factor receptor autophosphorylation sites do not stringently define association motifs for several SH2-containing proteins. *J Biol Chem* 1994;269:12320-12324.
39. Wyckoff JB, Insel L, Khazaie K, Lichtner RB, Condeelis JS, Segall JE: Suppression of ruffling by the EGF receptor in chemotactic cells. *Exp Cell Res* 1998;242:100-109.

Address reprint requests to:

Yama A. Abassi
 ACEA Biosciences Inc.
 11585 Sorrento Valley Rd., Suite 103
 San Diego, CA 92121

E-mail: yabassi@aceabio.com